THE PLANT CELL

Research Article

Manipulating *ZmEXPA4* expression ameliorates the drought-induced prolonged anthesis and silking interval in maize

Boxin Liu [1,2,3] Bin Zhang [1,4] Zhirui Yang [3] Yan Liu [3] Shiping Yang [3] Yunlu Shi [3,5] Caifu Jiang [3,5] and Feng Qin [3,5,*,†]

1 Key Laboratory of Plant Molecular Physiology, Institute of Botany, Chinese Academy of Sciences, Beijing 100093, China
2 University of Chinese Academy of Sciences, Beijing 100049, China
3 State Key Laboratory of Plant Physiology and Biochemistry, College of Biological Sciences, China Agricultural University, Beijing 100193, China
4 Beijing Vegetable Research Center (BVRC), Beijing Academy of Agriculture and Forestry Sciences (BAAFS), Beijing, 100097, China
5 Center for Crop Functional Genomics and Molecular Breeding, China Agricultural University, Beijing 100193, China

*Author for correspondence: qinfeng@cau.edu.cn
†Senior author
B.L., B.Z., Z.Y., Y.L., and Y.S. performed the experiments and analyzed the data. S.Y. helped perform genomic data analysis. C.J and F.Q. discussed and interpreted the data. B.L. and B.Z. drafted the manuscript. F.Q. conceived and advised on all the experiments and revised the manuscript.
The authors responsible for the distribution of materials integral to the findings presented in this article in accordance with the policy described in the Instructions for Authors (www.plantcell.org) is: Feng Qin (qinfeng@cau.edu.cn).

Abstract

Drought poses a major environmental threat to maize (*Zea mays*) production worldwide. Since maize is a monoecious plant, maize grain yield is dependent on the synchronous development of male and female inflorescences. When a drought episode occurs during flowering, however, an asynchronism occurs in the anthesis and silking interval (ASI) that results in significant yield losses. The underlying mechanism responsible for this asynchronism is still unclear. Here, we obtained a comprehensive development-drought transcriptome atlas of maize ears. Genes that function in cell expansion and growth were highly repressed by drought in 50 mm ears. Notably, an association study using a natural-variation population of maize revealed a significant relationship between the level of *α-expansin4* (*ZmEXPA4*) expression and drought-induced increases in ASI. Furthermore, genetic manipulation of *ZmEXPA4* expression using a drought-inducible promoter in developing maize ears reduced the ASI under drought conditions. These findings provide important insights into the molecular mechanism underlying the increase in ASI in maize ears subjected to drought and provide a promising strategy that can be used for trait improvement.

Introduction

Water scarcity and the unpredictable nature of drought threaten maize (*Zea mays*) production worldwide ([Daryanto et al., 2016](); [Gupta et al., 2020]()). Maize is the only monoecious plant among the major cereal crops and develops male and female inflorescences at different positions of the

same plant. The male inflorescence (tassel) is located at the top of the plant and develops from the apical meristem, while the female inflorescence (ear) is located in the middle of the plant and develops from a lateral meristem in a leaf axil. Anthesis occurs when pollen is disseminated from the tassel. Concomitantly, each gynoecium on the female

Open Access

IN A NUTSHELL

Background: Maize is the only monoecious plant among the major cereal crops. Maize develops male and female inflorescences at different positions of the plant. The male inflorescence (tassel) is located at the top, while the female inflorescence (ear) grows in the middle of a plant. Anthesis occurs when pollen is released from the tassel. Usually at the same time, pistils with long stigmas (silks) protrude from the ear bracts for pollination, a process referred to as silking. When a drought episode occurs during flowering, however, it leads to a significantly prolonged interval of anthesis and silking (ASI). Such an extension hampers successful pollination and greatly reduces yields.

Question: We want to know the molecular mechanism underlying why drought induces a prolonged ASI in maize. Is it possible to relieve this problem through genetic engineering?

Findings: Microscopic observation showed that drought stress had little effect on the development of tassels but markedly delayed ear growth. Moreover, when ears of the same developmental stage or size grown under well-watered and water deficit stress conditions were compared, the expression of genes related to flower organ differentiation and formation was rarely affected by drought. By contrast, genes functioning in cell expansion were significantly repressed by drought in 50 mm ears, which is probably implicated in the reduction in ear growth and silk elongation. Notably, an association study using a natural-variation population of maize revealed a significant relationship between the level of α-expansin4 (*ZmEXPA4*) expression and drought-induced prolonged ASI. Furthermore, genetic manipulation of *ZmEXPA4* expression using a drought-inducible promoter in developing maize ears reduced drought-induced prolonged ASI.

Next steps: In addition to the reduced cell expansion and growth in 50 mm ears under drought stress, which was revealed in this study, we also observed that the transition of axillary meristems from vegetative to floral identity was delayed by drought. We are interested in identifying the molecular mechanism underlying this phenomenon.

inflorescence forms a pistil with a long stigma (silk) that protrudes from the inflorescence bracts and becomes receptive to pollination, a process referred to as silking. The synchronous development of a tassel and ear is essential for pollination and seed set. When drought occurs during reproductive development, however, it typically results in asynchronous development of a tassel and ear, which leads to a significantly extended anthesis and silking interval (ASI). Such an extension hampers successful pollination and greatly reduces yields (Bolaños and Edmeades, 1996; Bruce et al., 2002). Thus, water deficit during flowering exerts a very strong detrimental effect on maize grain yield. Although it remains unclear why an extended ASI is induced by drought, selection for early vigorous silking has been pursued in maize breeding programs and is considered to be a beneficial trait for seed formation, especially under drought stress that occurs during flowering (Bruce et al., 2002).

Tassels and ears initially undergo a similar developmental program but eventually develop into distinct architectures during the following stages: (1) Inflorescence meristem (IM) stage—when the shoot apical and axillary meristems elongate and transform into tassel and ear inflorescence primordia; (2) Spikelet pair meristem (SPM) and spikelet meristem (SM) stage—when SPMs arise from the flank of the IM and each SPM develops into a pair of SMs; (3) Floret differentiation (FD) stage—when each spikelet in tassels develops into two flowers. In developing ears, however, the lower flower is aborted, and only the upper flower continues to develop into a functional flower with a functional ovary and silk; (4) Floral organ maturation (FM) stage—when the gynoecium primordia in tassel florets degenerate and the stamen primordia in ear

florets are aborted, which results in unisexual floral formation; (5) Silk elongation (SE) stage—when silks in ear florets rapidly elongate and protrude out of the inflorescence bracts to receive the pollen shed from tassel florets located on the top of the plant (Thompson and Hake, 2009; Tanaka et al., 2013).

In this study, we investigated the effects of drought on the development of male and female inflorescences in maize under four levels of water availability. We generated and comprehensively analyzed an ear drought-development transcriptome atlas. Importantly, genetic manipulation of α-expansin4 (*ZmEXPA4*) expression in developing ears using a drought-inducible promoter alleviated the drought-induced extension of the ASI.

Results

Ear development and growth are significantly delayed by drought

We carefully compared the developmental progress of tassels and ears under well-watered (WW) and water stress (WS) conditions to determine the effect of drought on inflorescence development. The relative soil water content (SWC) was maintained in a range of 35%–50% under WW treatment, while it was maintained at ~20% under WS treatment (Figure 1A). These conditions were maintained from the vegetative 5 (V5) to the V14 stage of development. During this period, the shoot apical meristems developed into tassels and went to anthesis, and axillary meristems developed into ears and went to silking. There were no obvious differences in the morphology and size of tassels in plants grown under WW and WS conditions, except that growth appeared to be slightly slower in V9–V11 under WS;
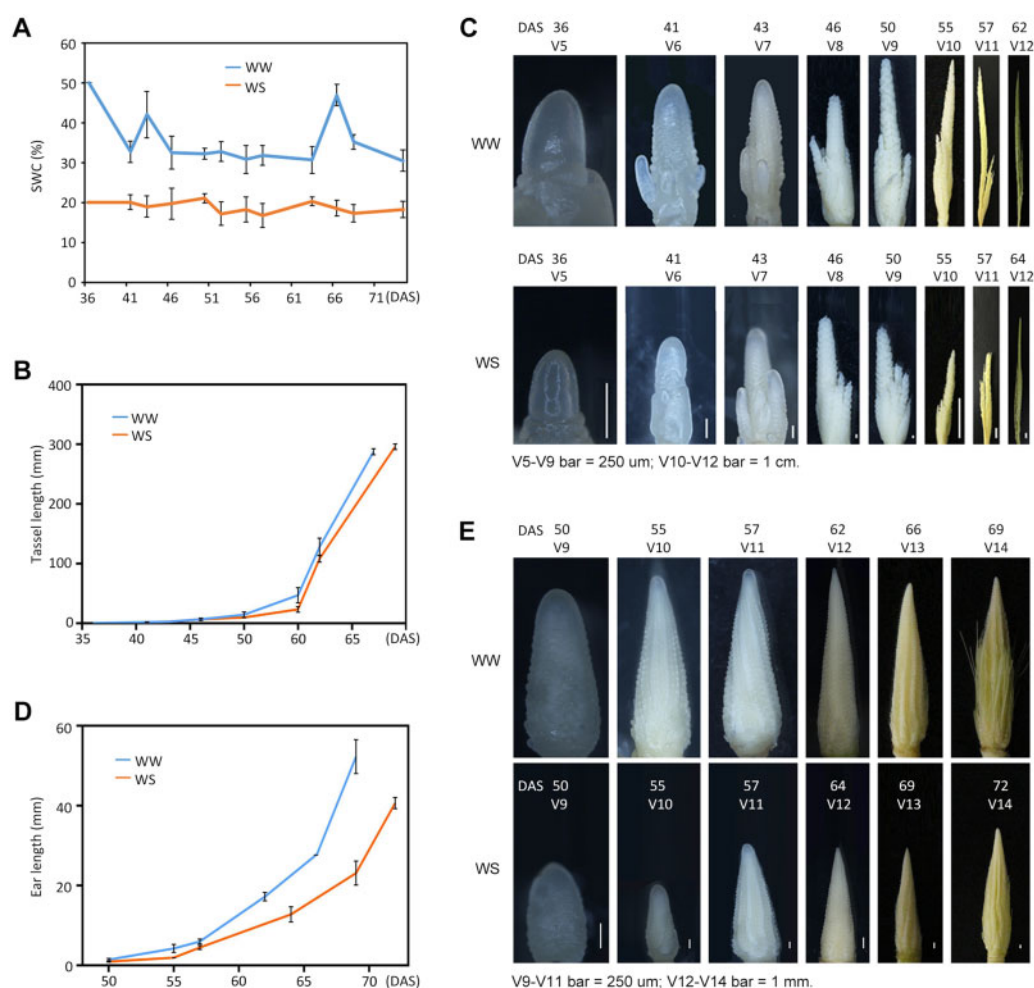
Figure 1 Observation of the development and growth of tassels and ears under WW and WS. A, Relative SWC was monitored from 36 to 76 DAS under the WW and WS treatments. Values represent mean ± SD from at least five field positions. B, The length of tassels from V5 (the fifth leaf with a visible ligule) to V12 under WW and WS conditions. C, Representative microscopic photographs of tassels under WW and WS conditions. D, The length of ears from V9 to V14 under WW and WS conditions. Values represent mean ± SD from at least three individual plants in (B) and (D). E, Representative microscopic photographs of ears under WW and WS conditions. The DAS and developmental stages are denoted above each photograph in (C) and (E). For each developmental stage, the tassel and ear from the same plant were measured. Representative photographs from at least three individual plants are shown.

however, the tassels attained the same length as those grown under WW conditions by V12 (Figure 1, B and C). Notably, however, clearly evident developmental retardation and growth reduction were observed in ears grown under WS conditions (Figure 1, D and E). When the V9 ear meristems of plants grown under WW conditions entered the SPM stage, ear meristems in WS plants were at the IM stage. When the silks of ears at V14 in WW plants were ~40 mm long, they were just emerging in plants under WS conditions (Figure 1, D and E). Collectively, these data indicate that the development and growth of ears were clearly more delayed by drought compared to tassels. This ultimately led to an asynchronism in anthesis and silking, thereby increasing the ASI. In addition, ears of comparable size were found to be in the same developmental stage in plants under WW and WS conditions, and drought-stressed ears eventually underwent all floral developmental processes without any evident floral organ defects or changes in ear architecture.

Development of a transcriptome atlas of maize ears under four watering regimes

To dissect how maize ears respond to drought, we analyzed the ear transcriptomes of B73 (a maize reference accession) grown under four watering regimes. The transcriptomes were derived from plants grown in the field under a rain-off shelter with a retractable dome and a drip-irrigation system to duplicate real field conditions. This arrangement allowed us to control SWC and allowed the plants to be exposed to normal radiation conditions and wind agitation (Supplemental Figure S1). Plantings were subjected to four different watering regimes by supplying an appropriate amount of water. The watering regimes were as follows: WW (SWC = 35%–30%); WS1 (SWC = 30%–25%); WS2 (SWC = 25%–20%); and WS3 (SWC = 25%–15%) (Figure 2A). Under WW, the time of anthesis coincided with silking, which began ~63 days after sowing (DAS) and finished at 68 DAS. A modest delay in anthesis was observed
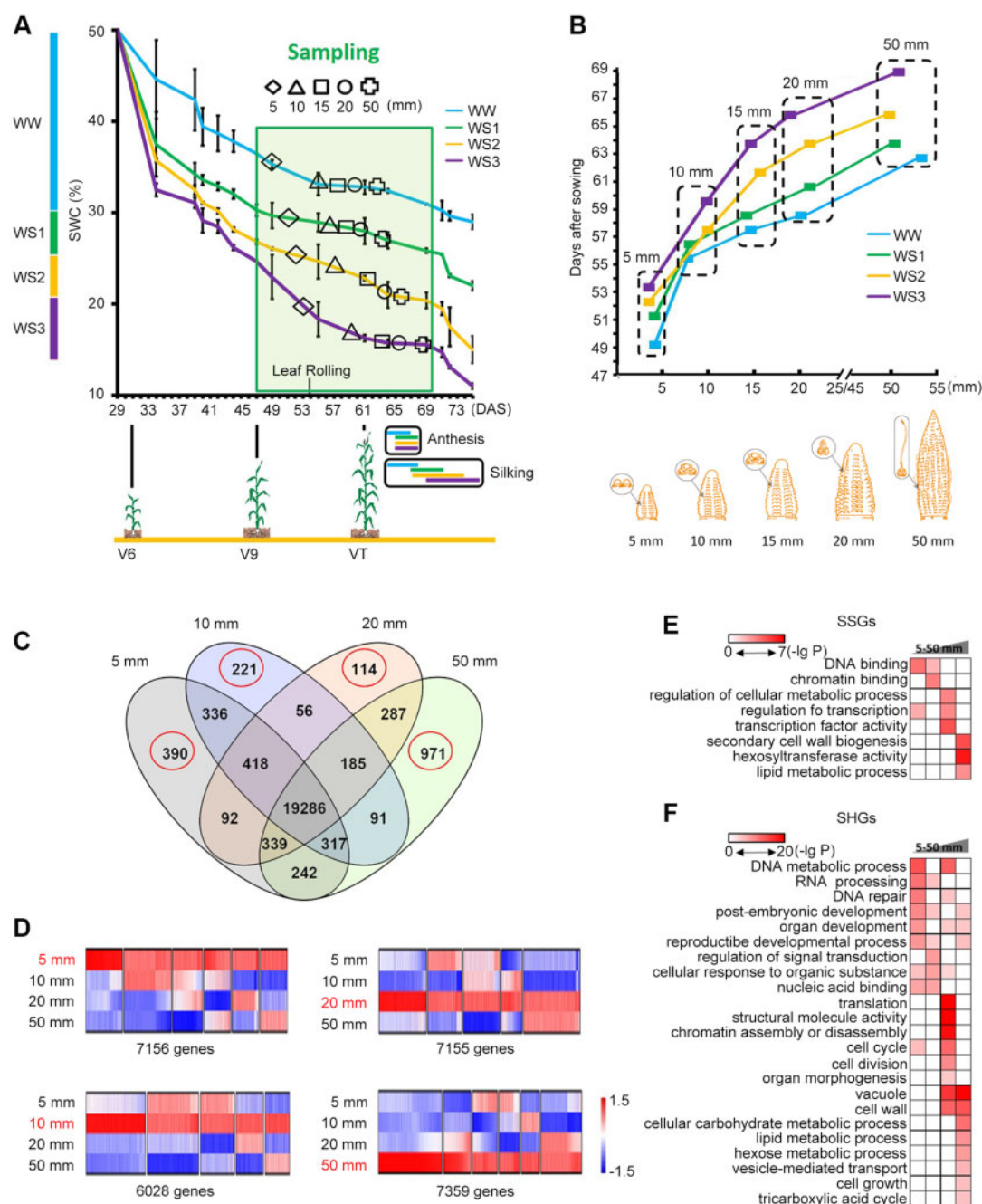
Figure 2 Transcriptome atlas of development and drought responses in maize ears. A, WS regimes established under field conditions. SWC under four watering regimes during plant growth and development. Values represent mean ± SD from at least five field positions. B, Date of ear sampling and corresponding ear size under the four watering regimes. Top: relationship of ears size to DAS under the four watering regimes. Bottom: schematic diagram of ear development at five sampling points. C, Venn diagram of gene expression in 5–50 mm ears. Red circle indicates the number of SSGs expressed during different developmental stages. D, Gene clusters of SSGs and SHGs (genes that were highly expressed at specific developmental stages). The bar color indicates gene expression level, which was normalized by the Z-score of gene expression across all samples. E and F, GO enrichment analysis of SSGs (E) and SHGs (F).

under drought conditions imposed by the restricted watering regimes. In contrast, however, the date of silking was significantly delayed in response to the drought stress regimes, with the extent of delay becoming more severe as drought stress increased. Silking began at 69 DAS under the WS3 regime, by which time anthesis had already been completed (Figure 2A). Samples were collected based on ear size rather

than days of growth to avoid transcriptomic alterations due to developmental discrepancies resulting from the different watering regimes. A dissecting microscope was needed to assist in the sampling of axillary meristems (Figure 2B). The sampling dates were adjusted in accordance with the stress levels, and analysis of the collected samples confirmed the observation that ear growth and development were delayed

by drought (Figure 2B). Different levels of drought-induced leaf rolling, reduced plant height, and grain yield were also observed and were proportional to the level of imposed drought (Supplemental Figure S1).

We analyzed the transcriptomes of 20 samples of ears of 5 different sizes, grown under 4 different WS regimes, with two independent biological replicates. On average, 55 million high-quality, pair-end reads were generated for each sample and mapped to the maize B73 reference genome (Jiao et al., 2017) (Supplemental Figure S2). The Pearson correlation coefficient of Fragments Per Kilobase of transcript per Million (FPKM) fragments mapped value of the two independent biological replicates was 0.98. Principal component analysis (PCA) indicated that the 20 samples clustered into four groups, with the 10 and 15 mm samples clustering together, indicating that their transcriptomes shared a high degree of similarity (Supplemental Figure S2). Therefore, these two datasets were merged and designated as the 10 mm sample in subsequent analyses. The four groups generally represented the developmental stages SPM and SM (2–5 mm), FD (10 and 15 mm), FM (20 mm), and SE (50 mm), indicating that the development had a more dominant effect than drought treatment on the ear transcriptome (Supplemental Figure S2).

Since development plays a predominant role in determining the ear transcriptome, we identified stage-specific genes (SSGs) and stage-highly expressed genes (SHGs; genes that were highly expressed at specific stages) present during the four different developmental stages. A total of 390, 221, 114, and 971 genes were identified as SSGs, and 7,156, 7,155, 6,028, and 7,359 were characterized as SHGs in the four different developmental stages, respectively (Figure 2, C–D; Supplemental Data Sets S1 and S2). Gene ontology (GO) enrichment analysis of SSGs and SHGs in 5 and 10 mm ears revealed a high level of DNA replication and transcription processes in these stages (Figure 2, E–F). A large number of SSGs and SHGs in the 20 mm ears were annotated with functions related to transcription and translation regulation, chromatin assembly, and organ morphogenesis, implying that active cell division and differentiation were occurring at this developmental stage (Figure 2, E–F). In contrast, genes related to cell wall biogenesis, vacuoles, and lipid and hexose metabolism were significantly enriched in 50 mm ears, indicating that rapid cell growth and expansion were occurring during this stage (Figure 2, E and F). Genes involved in organ development and reproductive processes were also enriched in SHGs during all stages of development.

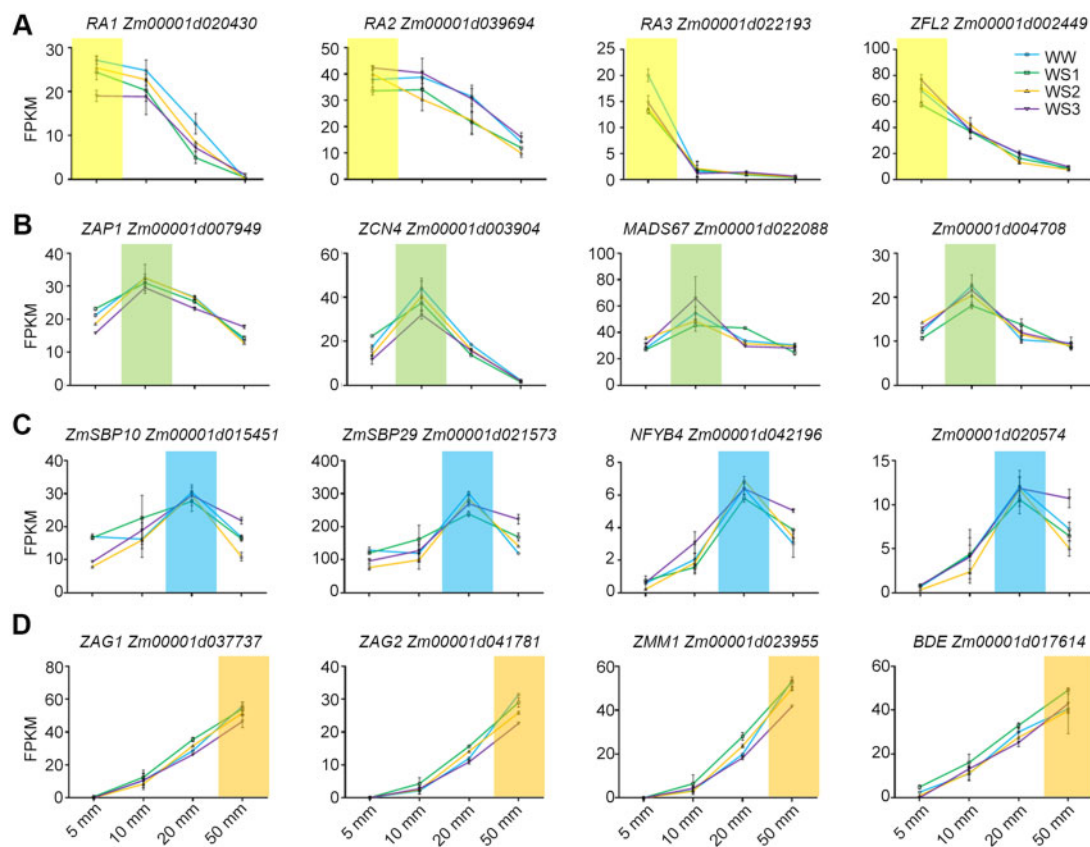**Figure 3** Expression patterns of genes that function in inflorescence development and SHGs under different watering regimes. Genes expressed in 5 mm (A), 10 mm (B), 20 mm (C), and 50 mm (D) maize ears. Data represent the mean ± SD of gene expression levels obtained from the replicated RNA-seq analyses. The colored bar highlights the developmental stage when the gene reaches the maximum expression level.

Developmental and floral organ identity genes are rarely affected by drought

We were interested in determining if the expression of development-related genes was affected by drought stress. Therefore, we examined the expression profiles of several gene reported to be involved in inflorescence differentiation and some identified SHGs within our development-drought atlas. *Ramosa1*, *Ramosa2*, and *Ramosa3* play integral roles in determining ear meristem size (Vollbrecht et al., 2005; Bortiri et al., 2006; Satoh-Nagasawa et al., 2006). Consistent with their functions in early ear development, these genes were highly expressed during very early stages and decreased in expression during later stages of ear development, further confirming the reliability of our sampling and transcriptome analysis. Importantly, however, their expression patterns were not altered in any evident manner in response to the different levels of drought stress (Figure 3A).

ZFL2, a maize homolog of *Arabidopsis thaliana* *FLORICAULA/LEAFY*, which functions in ear inflorescence architecture and floral organ patterning (Bomblies et al., 2003), was highly expressed in 5 mm ears, and its expression was not altered by drought stress (Figure 3A). *ZCN4* (encoding a florigen-like protein), *MADS67* and *ZAP1*, which function in the floral transition (Mena et al., 1995; Sun et al., 2020), and *Zm00001d004708* (function unknown) were highly expressed in 10 mm ears, but again different levels of drought stress had little effect on their expression (Figure 3B). Genes encoding Squamosa-promoter Binding Proteins (ZmSBP10 and ZmSBP29) and NFYB4 were highly expressed in 20 mm ears and exhibited little variation in expression in response to the four levels of water deficit (Figure 3C). Similarly, the expression of MADS box genes involved in floral organ identity, including *ZAG1*, *ZAG2*, *ZMM1*, and *BDE* (Schmidt et al., 1993; Theißen et al., 1995; Thompson et al., 2009; Smith and Zhao, 2016) gradually increased during ear development from 5 to 50 mm, reaching a maximum level of expression in 50 mm ears. Different levels of WS had little effect on the expression of these genes (Figure 3D). Collectively, the transcriptomic data indicate that the expression of these genes is largely dependent on developmental stage and is unaffected by drought. As long as ears developed to a certain stage, the genes were programmed to be expressed, regardless of drought conditions. The data support the premise that drought rarely alters ear inflorescence architecture in maize, except for prolonging the ASI.

Drought represses gene expression predominantly in 50 mm ears

Distinct from the above-mentioned genes, the expression patterns of a large number of genes were greatly altered by drought, as revealed by the development-drought transcriptomic analysis. To simplify our analysis of the effects of drought on gene expression, we considered genes whose expression was higher under the three drought conditions than under WW treatment to be upregulated genes in maize ears. Correspondingly, genes whose expression under the three drought conditions was lower than under WW treatment were regarded as genes that were downregulated by drought. As a result, 2,449, 3,815, 3,094, and 5,899 genes were identified as either upregulated or downregulated genes in response to drought in 5, 10, 20, and 50 mm ears, respectively. This represented 32%, 52%, 51%, and 71% of the SHGs and SSGs in ears of the respective size (Figure 4A; Supplemental Figure S3). The number of downregulated genes by drought was greater than the number of upregulated genes in maize ears at all four developmental stages. Downregulation in gene expression was the most predominant in 50 mm ears, accounting for 59% of SHGs and SSGs at this stage. We sorted the expression patterns into different clusters using a k-means clustering algorithm and annotated significantly enriched GO terms in each cluster. Collectively, these genes were related to auxin signaling, photosynthesis, cell wall, membrane integrity, and mitochondrial respiration (Figure 4A).

We further analyzed the expression profiles of key genes in the auxin signaling pathway to more fully characterize the changes in gene expression occurring in this pathway in 50 mm ears. Maize homologs encoding auxin receptors (Transport Inhibitor Response 1/Auxin Signaling F-box, TIR1/AFBs), auxin response factors (ARFs), and Small Auxin Upregulated RNAs (SAURs) were identified based on sequence homology with Arabidopsis genes. Our analysis indicated that the expression of all three maize *TIR1/AFBs*, and most *ARFs* (70%, 21/30), was not repressed by drought (Supplemental Figure S4). Among the 38 expressed *SAURs* in 50 mm ears, however, 27 genes were downregulated by different levels of drought stress and were significantly enriched among all the expressed genes ($P = 1.98\text{e-}5$, Fisher's exact test) (Figure 4B). Many of the photosynthesis-related genes were downregulated by drought. Genes associated with the photosynthesis electron transport chain, such as cytochrome b6/f complex, photosystem I and ATP synthase, and part of the photosystem II, were all repressed by drought (Figure 4A; Supplemental Figure S4). The expression of genes involved in the biosynthesis of the major substrates of cell wall polysaccharides, such as UDP-D-glucose, G-1-P, UDP-L-rhamnose, UDP-D-galacturonic acid, UDP-D-xylose, UDP-L-arabinose, GDP-D-mannose, GDP-L-fructose, and others, was also coordinately downregulated by drought in 50 mm ears (Figure 4C).

SAUR gene expression, carbon resources, and cell wall biogenesis play integral roles in cell growth and expansion (Spartz et al., 2014; Ren and Gray, 2015; Verbancic et al., 2018) and floral organ enlargement, especially in the rapid extension of silks, which are key processes that occur during this developmental stage. Therefore, we were interested in determining if the expression of genes directly involved in cell expansion was affected in drought-stressed 50 mm ears. Expansins and xyloglucan endotransglycosylases (XETs) function in reducing cell wall constraint and changing cell wall extensibility (Cosgrove, 2000, 2005). Aquaporins in stigmatic papilla cells play an important role as water channels (Dixit
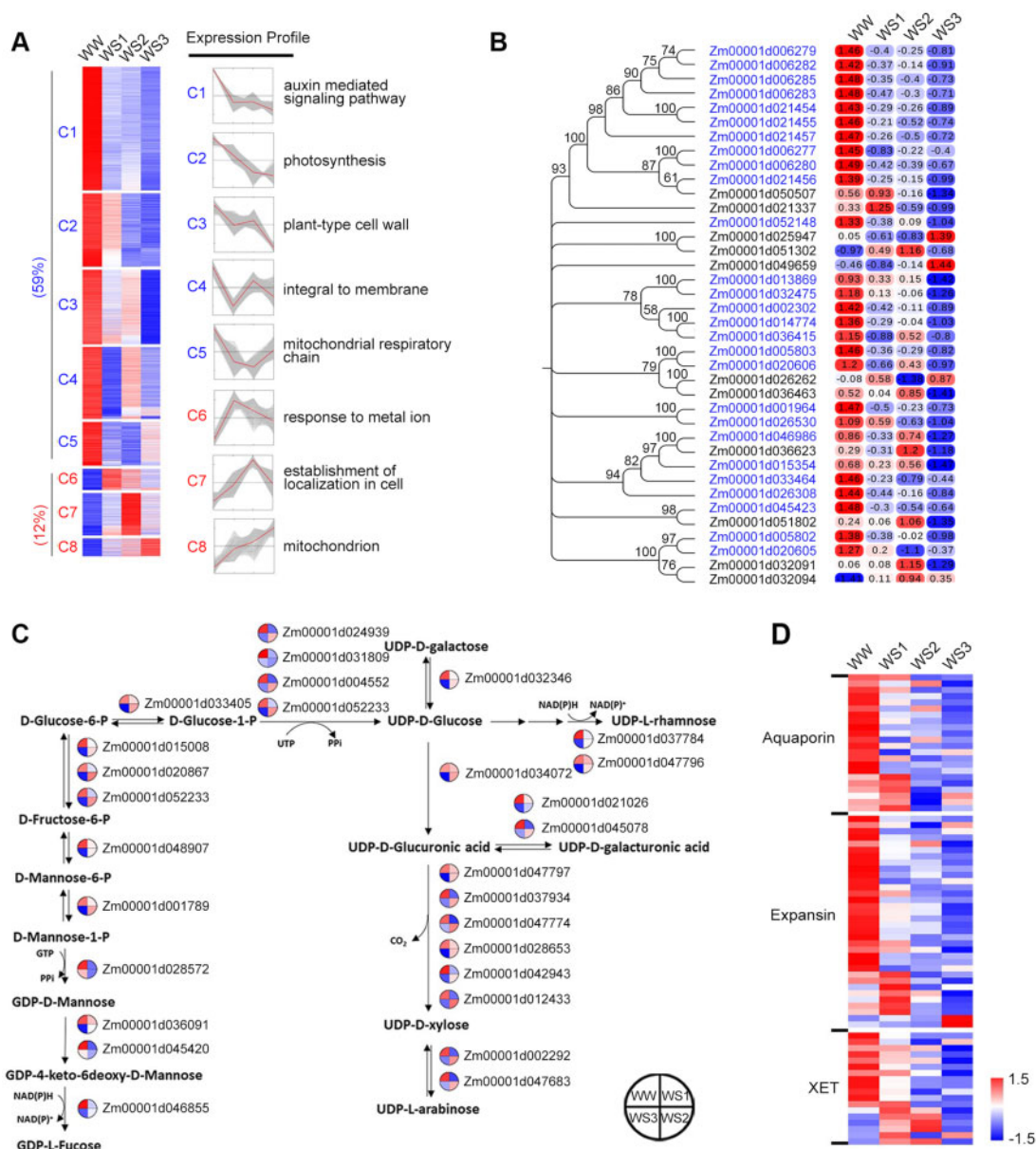
Figure 4 Drought-repressed gene expression in 50 mm ears. A, Drought-responsive expression profiles of SSGs and SHGs in 50 mm ears that exhibit different clustering patterns. Numbers on the left of each panel denote the percentage of downregulated (blue) and upregulated (red) genes. Gene expression profiles of individual genes are depicted in gray, and the average expression pattern for each cluster is depicted with a red line. The most significantly enriched GO term for each cluster is shown on the right side. B, Drought-responsive expression profiles of *SAUR* genes expressed in 50 mm ears. Left: phylogenetic tree of *SAUR* genes expressed in 50 mm ears. The bootstrap values are indicated at the nodes. Right: *SAUR* gene expression in responsive to WS. The numbers are the Z-score values of FPKM of each gene obtained from RNA-seq analysis. C, Genes encoding enzymes catalyzing the biosynthesis of cell wall precursors were downregulated by drought. The metabolic pathway was derived from MapMan (version 3.6.0), and the genes encoding the enzyme catalyzing each reaction were searched in the B73 genome based on homology to Arabidopsis genes. The expression levels of genes under WW, WS1, WS2, and WS3 treatments are shown in the top left, top right, bottom right, and bottom left corner of each pie, respectively. D, Expression profiles of *Aquaporin*, *Expansin*, and *XET* genes expressed in 50 mm ears under four different watering regimes. The bar color denotes the Z-score of the FPKM of each gene under each of the four treatments.

et al., 2001; Zhou et al., 2017), where they increase the permeability of the cell to allow a rapid influx of water to drive cellular expansion (Chaumont et al., 1998; Ehlert et al., 2009). A sequence homology survey of the maize genome identified 108 *Expansin* and 34 *XET* genes. Among these *Expansin* genes, 34 were expressed in 50 mm ears, 25 of which were downregulated by drought ($P = 1.54e-5$,

Fisher's exact test). Among the 18 *XET* genes expressed in 50 mm ears, 11 were downregulated ($P = 3.19e-2$, Fisher's exact test) (Figure 4D). Additionally, among the 22 *Aquaporin* genes expressed in 50 mm ears, 16 were downregulated and were significantly enriched among all the expressed genes ($P = 6.92e-5$, Fisher's exact test) (Figure 4D).

To validate the fidelity of the gene expression profiles obtained by RNA-seq analysis, we performed RT-qPCR to analyze the expression of 20 *Aquaporin* and *Expansin* genes whose expression was identified as downregulated by drought in the RNA-seq data. The average correlation coefficient between RNA-seq and RT-qPCR analyses was 0.94, indicating that the RNA-seq results were reliable (Supplemental Figure S5). Collectively, these data indicate that drought is a predominant driver of gene repression in 50 mm maize ears, which may result in reduced or delayed cell growth and expansion.

Natural variation in *ZmEXPA4* is associated with ASI under drought stress

We performed candidate gene association analysis using a natural variation population consisting of 228 maize accessions to explore the potential contributions of the identified downregulated genes to drought-induced extended ASI during flowering. The genotypes in the population were mainly collected from temperate regions and share a similar flowering time. Data on the phenotypic variation in ASI under WW and WS conditions were obtained in Beijing, China (under a rain-off shelter) in 2016 and in Xinjiang, China in 2017 and 2018 where rainfall was very scarce. The repeatability (h^2) of day to anthesis, day to silking, and ASI in response to WW and WS conditions at the three locations was in the range of 0.71–0.86 (Supplemental Figure S6). We performed association analyses of the 104 downregulated genes in 50 mm ears, including *Aquaporins*, *Expansins*, *XETs*, photosynthesis-related genes, and genes involved in cell wall biosynthesis. We also characterized the genetic diversity of 2,709 high-quality single-nucleotide polymorphism (SNP) markers (minor allele frequency ≥0.05, missing rate <0.2) for these genes in the population (Liu et al., 2017; Liu et al., 2020).

Only a synonymous SNP1875, located in the last exon of *ZmEXPA4* (Zm00001d034663), was significantly associated with the ASI phenotype. The significance of SNP1875 was confirmed by reanalyzing the genomic variation, including SNPs and small insertions/deletions based on 20× coverage genome-resequencing data (Yang et al., 2019). Three additional significant SNPs were identified. One of these SNPs is located in the last intron and two reside in the downstream of 3′-untranslation region (3′-UTR) of *ZmEXPA4*, implying that these variations are likely associated with the ASI phenotype by affecting the expression of this gene (Supplemental Figure S7).

Thus, we analyzed the expression of *ZmEXPA4* in 50 mm ears among 52 maize inbred lines grown under WW and WS conditions. Drought-induced ASI was negatively correlated with the ratio of *ZmEXPA4* expression under WS to WW conditions, but was not directly correlated with the expression of this gene under either WW or WS conditions alone (Supplemental Figure S7). Accessions with the C genotype of SNP1875 had a higher WS/WW expression ratio and exhibited a shorter ASI compared to accessions with the G

genotype (Supplemental Figure S7). These data suggest that maintaining a higher level of *ZmEXPA4* expression may alleviate the prolonged ASI under drought conditions, although the causal variation awaits further characterization.

Genetic engineering of *ZmEXPA4* expression in developing ears reduces ASI under drought conditions

Based on the results of the association analysis, we explored whether the use of a drought-inducible or constitutive highly expressed promoter to drive *ZmEXPA4* expression in developing ears would improve the ASI trait. The promoters of two genes were selected based on our ear RNA-seq data. *Zm00001d039566* expression was identified as highly drought inducible, while *Zm00001d045478* was highly expressed in 50 mm ears under WW conditions with only a minor level of upregulation under drought conditions (Figure 5A; Supplemental Figure S8). Approximately 2-kb promoter fragments of both genes were cloned and separately inserted in front of *ZmEXPA4*. Subsequently, two types of transgenic maize were generated using these constructs (abbreviated as 566pro and 478pro) (Figure 5B). We evaluated the transgenic expression of each construct in two independent transformation events.

The expression level of *ZmEXPA4* was ~20-fold higher in 566pro plants than in nontransgenic, wild-type (WT) plants, and its expression level doubled under drought conditions (Figure 5C). In contrast, the expression of *ZmEXPA4* in 478pro plants was 40–150 times greater than the WT under WW conditions, but it was not inducible under WS conditions (Figure 5D). Immunoblot analysis confirmed the drought-inducible accumulation of ZmEXPA4-Myc protein in 566pro transgenic plants (Figure 5E). No obvious differences in ASI or plant height were observed between WT and the four transgenic lines under WW conditions (Figure 5, F and G). Notably, however, the two independent lines of 566pro plants exhibited a significant reduction in ASI under drought conditions. The average ASI was 6.03 days in WT plants and 4.04 days in 566pro plants. In contrast, no significant difference in ASI was observed between WT and 478pro plants under drought conditions (Figure 5, H and J). All WT and transgenic plants had similar plant height under WS conditions (Figure 5I). In addition to early vigorous silking, the ears of 566pro plants exhibited a tendency to stretch out of the bracts under WS but not WW conditions (Supplemental Figure S8). We did not notice any yield penalty in either 478pro and 566pro transgenic plants compared with WT under both WW and WS conditions (Supplemental Figure S9). Whether manipulating *ZmEXPA4* expression would achieve final yield gains requires further field tests.

Discussion

In this study, we investigated tassel and ear growth and development in maize under WW and WS conditions and found that ear growth was significantly delayed by drought
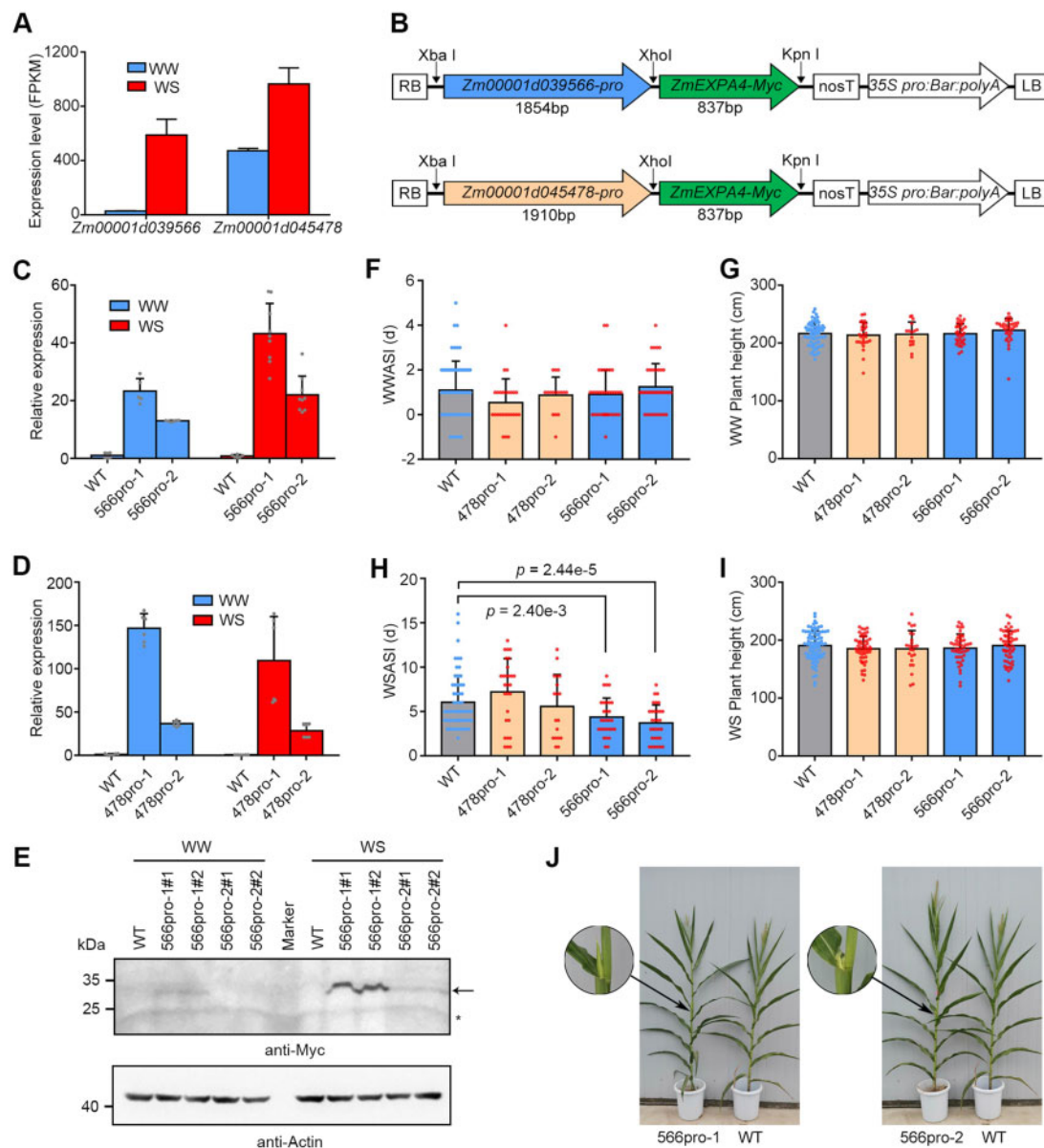
Figure 5 Genetic engineering of *ZmEXPA4* expression in developing ears reduces ASI under drought conditions. A, FPKM values of *Zm00001d039566* and *Zm00001d045478* under WW and WS conditions, obtained by RNA-seq analysis. B, Schematic diagram of the T-DNA region of the two constructs that utilized promoter fragments from *Zm00001d039566* and *Zm00001d045478* to drive *ZmEXPA4* expression, respectively. C, Transcript levels of *ZmEXPA4* in WT and two independent *Zm00001d039566pro:ZmEXPA4* transgenic lines (566pro-1 and 566pro-2) and plants grown under WW and WS conditions. D, Transcript levels of *ZmEXPA4* in WT and two independent *Zm00001d045478pro:ZmEXPA4* transgenic lines (478pro-1 and 478pro-2) under WW and WS conditions. The expression level of *ZmEXPA4* in WT plants under WW conditions was defined as "1" in (C) and (D). Values represent mean ± SD ($n > 4$). E, Immunoblot analysis of ZmEXPA4 protein levels in WT and 566pro-1 and 566pro-2 under WW and WS, detected with anti-Myc antibody. For each transgenic line, ears from two different plants (#1, #2) were analyzed. The equivalent sample loading was confirmed by detection with anti-Actin antibody. The arrow indicates the ZmEXPA4-Myc protein, and the asterisk indicates a nonspecific band. F–I, ASI (F) and plant height (G) under WW conditions; ASI (H) and plant height (I) under WS conditions. All plants were grown under rain-off shelters in the field. Data represent the mean ± SD of at least 30 plants for each line. Statistical significance was determined by a two-sided *t*-test. J, Representative photographs of 566pro-1 and 566pro-2 compared with WT plants grown under WS conditions. The magnified images show the emergence of the ear and silks on the transgenic plants when they were not visible on WT plants.

(Figure 1). Previous transcriptome studies sampled ear tissues under normal and drought stress conditions based on the same period of growth (DAS). This approach, however, captured the combined effects of drought on ear development and tissue-specific responses to stress (Miao et al.,

2017; Danilevskaya et al., 2019). PCA indicated that the stage of development is a greater determinant of the expressed transcriptome than drought stress (Supplemental Figure S2). Thus, a great number of differentially expressed genes would be identified that were related to the stage of development

if ears were sampled and compared based on DAS, since drought clearly delays ear growth and development. In this study, however, we collected samples based on ear size that corresponded to different developmental stages. This approach allowed us to exclude differences in gene expression that were due to stress-induced developmental retardation and instead identify genes that were more specifically related to the drought response. Using this approach, we provided evidence that genes that determine ear inflorescence architecture and floral organ identity are rarely affected by drought and that their expression patterns are largely programmed by developmental cues (Figure 3).

Drought quickly stimulates abscisic acid signaling and biosynthesis in leaves, which induces stomatal closure and inhibits gas exchange and photosynthesis (Zhu, 2016; Chen et al., 2020). A shortage of photo-assimilates would reduce the rate of cell growth, since UDP-D-glucose is the major building block for the synthesis of cell wall polysaccharides. Unexpectedly, a number of photosynthesis-related genes were highly expressed and downregulated by drought in 50 mm ears, when the ears and emerging silks were still wrapped by bracts and could not receive light (Supplemental Figure S4). Photosynthetic activity occurs in the hypocotyls of soil-grown common bean (*Phaseolus vulgaris*) plants due to light piping from the aboveground tissues and may contribute to its own carbon supply (Kakuszi et al., 2016). We reasoned that 50 mm ears and silks can acclimate to photosynthetic conditions. After the silks extend out of bracts and are exposed to direct light, their photosynthetic capacity may contribute to the carbon needed for rapid cell growth and expansion, as well as stigma activity, in addition to the photoassimilates provided via phloem transport from leaves. Thus, early vigorous silk extension from bracts would benefit SE and support effective pollination.
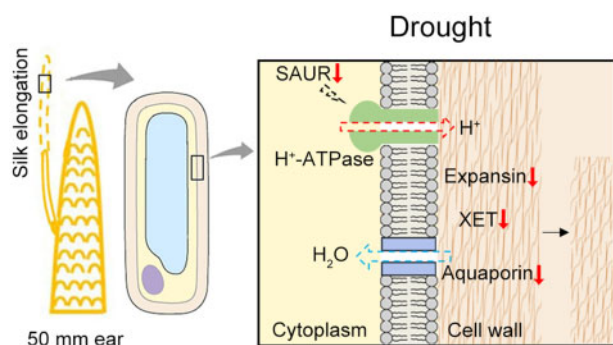

Figure 6 A proposed model for reduced SE under drought stress. Under favorable growth conditions, SAURs function as positive regulators of cell expansion by activating H^+-ATPase activity (Spartz et al., 2014), which triggers the acidification of the cell wall. Together with the functions of Expansins, XETs, and Aquaporins, rapid cell expansion of silks is achieved in developing ears. Drought represses the expression of these genes, resulting in reduced SE, which eventually leads to a drought-induced increase in ASI.

Genes encoding SAURs, expansins, XETs, and aquaporins were coordinately downregulated in drought-stressed 50 mm ears, indicating that cell elongation and growth are significantly repressed by drought. SAURs function as positive regulators of cell expansion by releasing the H^+-ATPase activity that was inhibited by D-clade type 2C protein phosphatases (Chae et al., 2012; Spartz et al., 2014). SAUR16 and SAUR50 promote hypocotyl elongation in the dark and enhance cotyledon expansion and opening in the light, depending on auxin levels (Sun et al., 2016; Dong et al., 2019). Expansin, which unlocks a network of wall polysaccharides, drives turgor-driven cell enlargement (Cosgrove, 2000). Immunofluorescence analysis indicated that ZmEXPA4-Myc is localized to the cell wall, supporting its function in the cell wall (Supplemental Figure S10). Aquaporin, a water-channel protein, contributes to adjustments in cell turgor, which also affect XET activity, and acting together, they synergistically induce cell growth (Wu et al., 2005; Lee et al., 2018). We propose that drought represses the expression of these genes, which has a negative impact on ear growth and SE, eventually leading to drought-induced extension of the ASI (Figure 6).

Two types of promoters, a drought-inducible promoter and a constitutive promoter that is highly expressed in 50 mm ears, were selected to drive ZmEXPA4 expression based on our ear development-drought transcriptome analysis. Although the expression of Zm00001d039566 was determined to be hundreds of times greater under WS versus WW conditions based on RNA-seq data, use of the 2-kb cloned promoter only enhanced ZmEXPA4 expression in transgenic maize plants ~20-fold under WW conditions and 40-fold under WS conditions. Perhaps a more suitable promoter fragment could be identified in future studies that will increase the expression of ZmEXPA4. Nevertheless, drought-induced prolonged ASI was alleviated in transgenic maize plants when ZmEXPA4 was driven by the drought-inducible promoter cloned from Zm00001d039566.

In contrast, ZmEXPA4 driven by a constitutive highly expressed promoter failed to improve the drought-inducible ASI trait. These results are consistent with the observation that a higher WS/WW expression ratio of ZmEXPA4 is associated with a reduced drought-induced ASI (fewer asynchronous days), but the absolute expression level of ZmEXPA4 under either WW or WS conditions is not (Supplemental Figure S7). We propose that drought represses the expression of ZmEXPA4 in WT plants. However, the modified ZmEXPA4 expression engineered in transgenic maize through the use of a drought-inducible promoter helped compensate for the reduction in ZmEXPA4 expression, which aided in the alleviation of drought-induced prolonged ASI. Plants with constitutive expression of this gene, however, may lack this resilience. Based on association analysis, we also propose that the identification of causal variants or the selection of plants with a higher WS/WW expression ratio of ZmEXPA4 may facilitate the improvement of this trait.

Collectively, this study provides a promising strategy for ameliorating the negative impact of drought-induced extended ASI in maize, which is detrimental to grain yield. Our data also suggest that the selection of an *ZmEXPA4* allele that maintains a high WS/WW expression ratio would be beneficial for trait improvement.

Material and Methods

Plant growth, WS treatment, and ear sampling

For the experiment comparing the developmental differences of ears and tassels under WW and WS conditions, ear sampling for RNA-seq analysis, and drought-induced ASI analysis of transgenic plants, *Z. mays* plants were grown in the field under a rain-off shelter in Beijing, China (40°N 116°E; 75 m above mean sea level [Amsl]). WS was applied by differential watering with a drip irrigation system. The relative SWC (v/v) was recorded every 2–3 Amsl days with a Field Scout^{TM} TDR 300 Soil Moisture Meter from 36 to 76 DAS (typically from V5 to V14). The relative SWC was maintained in a range of 3550% under WW treatment, when the water potential was approximately 0 to −30 AmslkPa (Watermark 200SS Sensor) (Jabro et al., 2020). For WS treatment, the relative SWC was kept at ∼20% (−140 to −160Amsl kpa). During this period of time, the amount of watering under WS treatment was ∼25%–30% that of WW treatment, depending on weather conditions. The shoot apical meristems experienced the stages of tassel primordia initiation to anthesis, and axillary meristems developed into ears and finished silking. The shoot apical and axillary meristems from tassels and ears were dissected and observed under a Nikon 80i Upright microscope from V5 to V12 for tassels and V9 to V14 for ears.

To obtain ear samples for RNA-seq analysis, four watering regimes were applied to the plants by differentially watering through a drip irrigation system, and SWC was recorded. The axillary meristems of the first developing ears were sampled. Ears of similar sizes (2–5, 10, 15, 20, and 50 mm long) obtained under different watering regimes were harvested and frozen immediately in liquid nitrogen for RNA preparation. To eliminate random effects, each sample was pooled from at least three individual plants, and two replicates were performed for RNA preparation and sequencing analysis.

RNA-sequencing, gene expression calling, and PCA

Total RNA was extracted from the samples using a TaKaRa MiniBEST Plant RNA Extraction Kit. RNA-seq libraries were constructed and sequenced by BerryGenomics to generate 150-nucleotide paired-end reads (Q30 > 86%) on the Illumina HiSeq4000 platform. The B73 reference genome (RefGen_version 4.38) was downloaded from http://plants.ensembl.org/Zea_mays/Info/Index (Jiao et al., 2017). Illumina sequencing reads were mapped to the B73 reference genome using HISAT2 version 2.1.0 with default settings. On average, ∼93% of reads were mapped to the genome, and 89% of reads were uniquely mapped. The bam files were used as inputs for StringTie version1.3.4d software, and FPKM fragments mapped values were calculated to measure the expression levels of genes with R-Ballgown (version 3.8) (Pertea et al., 2016). Genes with FPKM ≥ 1 were recognized as expressing genes in ears during a specific stage. PCA was performed using the prcomp function in R software with default settings to facilitate graphical interpretation of relatedness among the 20 different samples. SSGs were defined as genes with FPKM ≥ 1 only in one specific developmental stage. SHGs were filtered by Z-score >0.5 for a certain developmental stage. The Z-score for a gene at different developmental stages (or drought levels) was calculated by the formula: $(x - \mu)/\delta$, where x is the FPKM value of a gene at a specific developmental stage (or drought level), μ is the average FPKM value at the four developmental stages (or drought levels), and δ is the standard deviation of the FPKM values at the four developmental stages (or drought levels).

RT-qPCR analysis

Total RNA (2 μg) was reverse transcribed using oligo-dT primer and reverse transcriptase (Promega) following the manufacturer's instructions. Quantitative real-time Polymerase Chain Reaction (qPCR) was performed on an ABI StepOnePlus real-time PCR system using an SYBR Premix Ex Teq II kit (Takara Bio, Kyoto, Japan). One microliter cDNA was used as template in a 10 μL reaction volume. The qPCR program was as follows: melting at 95°C for 15 s, and amplification with 40 cycles of 95°C for 15 s and 60°C for 30 s. The measurements were obtained using the comparative CT ($2^{-\Delta\Delta CT}$) relative quantification method (Schmittgen and Livak, 2008). *ZmUbiquitin1* (*ZmUbi1*) was used as an internal control. The primers are listed in Supplemental Data Set S3.

Clustering of gene expression profile and GO enrichment analysis

The k-means method and MeV software were used for expression pattern clustering analysis. The figure of merit was used to determine the optimal cluster number (Yeung et al., 2001). GO enrichment annotation was performed based on AgriGO (Du et al., 2010; Tian et al., 2017). MapMan (version 3.6.0) and KEGG pathway analysis https://www.kegg.jp/kegg/pathway.html (Thimm et al., 2004; Usadel et al., 2009) were used to analyze cell wall biogenesis and photosynthesis-related genes.

Phylogenetic analysis

Amino acid sequences were retrieved from the MaizeGDB (https://www.maizegdb.org/). The full-length amino acid sequences of 38 *SAURs* expressed in 50 mm ears (Supplemental Data Set S4) were aligned and the phylogenetic tree was constructed based on this alignment using the neighbor-joining method in MEGA version X (http://www. megasoftware.net/) with the following parameters: Poisson correction, pairwise deletion, uniform rates, and

bootstrap (500 replicates). The tree file used for phylogenetic analysis is provided in Supplemental Data Set S5.

Phenotypic analysis of the drought-induced ASI in 228 maize accessions in the field

A total of 228 maize accessions originating from temperate regions were collected for this study. To investigate the drought-induced ASI phenotype, all of these materials were grown in 2016 in Beijing, China (40°N 116°E; 75 m Amsl) in the field under a rain-off shelter and in 2017 and 2018 in Urumchi, China (44°N 88°E; 619 m Amsl) in fields where the rainfall was very scarce. During the growing season (from May to August), the mean day length was ~14.4 and 14.8 h, the average temperature was ~30.2°C and 29.5°C, and the relative humidity was ~58% and 45% in Beijing and Urumchi, respectively. The plants were grown in a randomized complete block design, with two replications under WW conditions in 2016–2018, and two replications under WS in 2016–2017, and three replications in 2018. Thirteen seeds were sown in each row (3 m long) with a row-spacing of 0.25 m. WS was applied from the V5 (the fifth leaf with visible ligule) stage to the grain filling stage by controlled irrigation, which maintained the relative SWC at ~15%–20% (approximately −160 to −200 kPa). SWC was recorded by a Field Scout™ TDR 300 Soil Moisture Meter, and water potential was determined using a Watermark 200SS Sensor. Typically, irrigation was supplied approximately every 10 days, with ~150–225 tons of water applied/hectare each time, depending on the SWC. The dates of anthesis and silking for each plant were recorded. The date of anthesis was recognized when half of the anthers in a tassel shattered and shed pollen grains. The date of silking was recognized when silks visibly stretched out the bracts. Plant height was measured after anthesis. The correlation of any two phenotypes was analyzed using the pairs function in R. The phenotype was estimated by the best linear unbiased prediction (BLUP) based on the data obtained in the 3 years, and the repeatability of the phenotype based on broad-sense heritability (h^2) was calculated using the "lmer" function in the R package lme4 (Wang et al., 2016).

Candidate gene association analysis

Association analysis of the ASI under WS was conducted by MLM using the TASSEL software package (Bradbury et al., 2007). The population structure was calculated using ADMIXTURE (Alexander et al., 2009). In total, 2,709 SNPs were identified for 104 downregulated genes in 50 mm ears, including photosynthesis-related genes, cell wall biosynthesis genes, Aquaporins, Expansins, and XETs, based on the genotype data (Liu et al., 2020). Among these, 100 genes were polymorphic, with an average of 27 SNPs for each gene. Statistical significance was determined by Bonferroni correction at $P < 3.7e-4$ (1/2,709). Variant callings, including SNPs, insertions, and deletions (<50 bp), on an 8.3-kb genomic fragment of ZmEXPA4 gene, were performed as described by Yang et al. (2019). Pairwise LD analysis was performed using the R package LD heatmap package (version 0.99).

Generation of ZmEXPA4 transgenic plants and ASI analysis of these plants

The coding sequence of ZmEXPA4 with a Myc-tag was cloned into the pCAMBIA3300 vector. Approximately 2-kb promoter fragments of Zm00001d039566 and Zm00001d045478 were cloned and constructed in front of ZmEXPA4, respectively. The two plasmids were transformed into Agrobacterium tumefaciens EAH105 cells, which were used to transform immature embryos of maize inbred line LH244 via Agrobacterium-mediated transformation (Ishida et al., 2007). T0 plants harboring one or two copies of the T-DNA insertion were selected and self-pollinated to generate T1 seeds. Homozygous T2 lines were used for subsequent analysis. ZmEXPA4 expression in the transgenic lines was determined by RT-qPCR; ZmUbi2 was used as an internal control. The two types of transgenic plants and WT plants were grown in a field under a rain-off shelter and compared. WW and WS treatments were carried out by differential watering as described above. The time of anthesis and silking and plant height were recorded. The PCR primers used in this study are listed in Supplemental Data Set S3.

Immunoblotting analysis

Protein samples were mixed with the same volume of 2× protein loading buffer and boiled at 95°C for 10 min. The extracts were centrifuged at 12,000 g for 5 min, and the proteins in the extracts were separated by SDS–PAGE. PageRuler prestained Protein Ladder (Thermo Fisher Scientific, Waltham, MA, USA) was used as size standards. The proteins were transferred to PVDF membranes and detected with antibodies against Myc (Sigma, St Louis, MO, USA; M4439) and Actin (ABclonal, Woburn, MA, USA; AC009). Actin served as the loading control.

Immunofluorescence microscopy

Paraffin slides with silk or ear samples were deparaffinized and rehydrated. The slides were immersed in EDTA antigen retrieval buffer (pH 8.0) in a microwave oven for antigen retrieval. After removing the excess liquid, the target tissue was marked with a liquid blocker pen. Three percentage of BSA was added to cover the marked tissue to block nonspecific binding, and the sample was incubated for 30 min. After removing the blocking solution, the slides were incubated in Anti-c-Myc Rabbit pAb (GB13076; 1:200 dilution; Servicebio, Wuhan, China;) overnight at 4°C. The slides were washed 3 times (5 min each) with PBS (pH 7.4) in a rocker device and the liquid discarded. The target tissue was covered with Cy3 conjugated Goat Anti-Rabbit IgG (GB21303; 1:300 dilution; Servicebio), and the sample was incubated at room temperature for 50 min in the dark. The sample was washed 3 times with PBS (pH 7.4) and incubated in DAPI solution at room temperature for 10 min in the dark. After washing 3 times with PBS (pH 7.4), spontaneous fluorescence quenching reagent was added, and the sample was incubated for 5 min. The slide was washed with running water for 10 min. After removing excess liquid, the sample was covered with a cover slip with anti-fade mounting medium.

The samples were examined by fluorescent microscopy (NIKON Eclipse ci microscope) and photographed. Nuclei were stained blue with DAPI.

Statistical analysis

The *t* test and phyper functions in R were used for the two-sided Student's *t*-test and the Fisher's exact test, respectively. Details are shown in Supplemental Data Set S6.

Accession numbers

Sequence data from this article can be found in the GenBank libraries under the following accession number: *ZmEXPA4*: ONM10950.1. Additional accession numbers are listed in Supplemental Data Sets S1 and S2. The RNA-seq data from this article can be found in the Genome Sequence Archive under accession number PRJNA659061.

Supplemental data

The following materials are available in the online version of this article.

Supplemental Figure S1. Plant performance under different levels of drought stress under a rain-off shelter in the field.

Supplemental Figure S2. Sequencing data and clustering of the RNA-seq reads of 20 ear samples.

Supplemental Figure S3. Clustering of drought-responsive gene expression patterns in 5, 10, and 20 mm ears.

Supplemental Figure S4. Drought-responsive expression profiles of genes that function in photosynthetic reactions and auxin signaling in 50 mm ears.

Supplemental Figure S5. Comparison of the expression patterns of *Aquaporin* and *Expansin* genes determined by RT-qPCR and RNA-seq under different watering regimes.

Supplemental Figure S6. Phenotypic variation in drought-induced ASI among 228 maize accessions.

Supplemental Figure S7. Natural variation in *ZmEXPA4* is significantly associated with drought-induced ASI.

Supplemental Figure S8. Tissue-specific expression patterns of *Zm00001d039566* and *Zm00001d045478*.

Supplemental Figure S9. Yield traits of *ZmEXPA4* transgenic lines under WW and WS conditions.

Supplemental Figure S10. Immunolocalization analysis of ZmEXPA4-Myc protein in *Zm00001d039566pro:ZmEXPA4* transgenic plants.

Supplemental Data Set S1. SSGs in ears at four developmental stages under WW conditions.

Supplemental Data Set S2. SHGs in ears at four developmental stages under WW conditions.

Supplemental Data Set S3. Primers used in this study.

Supplemental Data Set S4. The amino acid sequences of 38 SAUR proteins.

Supplemental Data Set S5. Tree file used for phylogenetic analysis of SAUR proteins.

Supplemental Data Set S6. Student's *t*-tests results for each figure.

References

Alexander DH, Novembre J, Lange K (2009) Fast model-based estimation of ancestry in unrelated individuals. Genome Res **19**: 1655–1664

Bolaños J, Edmeades GO (1996) The importance of the anthesis-silking interval in breeding for drought tolerance in tropical maize. Field Crops Res **48**: 65–80

Bomblies K, Wang RLAmbrose BA, Schmidt RJ, Meeley RB, Doebley J (2003) Duplicate *FLORICAULA/LEAFY* homologs *zfl1* and *zfl2* control inflorescence architecture and flower patterning in maize. Development **130**: 2385–2395

Bortiri E, Chuck G, Vollbrecht E, Rocheford T, Martienssen R, Hake S (2006) *ramosa2* encodes a LATERAL ORGAN BOUNDARY domain protein that determines the fate of stem cells in branch meristems of maize. Plant Cell **18**: 574–585

Bradbury PJ, Zhang Z, Kroon DE, Casstevens TM, Ramdoss Y, Buckler ES (2007) TASSEL: software for association mapping of complex traits in diverse samples. Bioinformatics **23**: 2633–2635

Bruce WB, Edmeades GO, Barker TC (2002) Molecular and physiological approaches maize improvement for drought tolerance. J Exp Bot **53**: 13–25

Chae K, Isaacs CG, Reeves PH, Maloney GS, Muday GK, Nagpal P, Reed JW (2012) *Arabidopsis SMALL AUXIN UP RNA63* promotes hypocotyl and stamen filament elongation. Plant J **71**: 684–697

Chaumont F, Barrieu F, Herman EM, Chrispeels MJ (1998) Characterization of a maize tonoplast aquaporin expressed in zones of cell division and elongation. Plant Physiol **117**: 1143–1152

Chen K, Li GJ, Bressan RA, Song CP, Zhu JK, Zhao Y (2020) Abscisic acid dynamics, signaling, and functions in plants. J Integr Plant Biol **62**: 25–54

Cosgrove DJ (2000) Loosening of plant cell walls by expansins. Nature **407**: 321–326

Cosgrove DJ (2005) Growth of the plant cell wall. Nat Rev Mol Cell Biol **6**: 850–861

Danilevskaya ON, Yu G, Meng X, Xu J, Stephenson E, Estrada S, Chilakamarri S, Zastrow-Hayes G, Thatcher S (2019) Developmental and transcriptional responses of maize to drought stress under field conditions. Plant Direct **3**: e00129

Daryanto S, Wang L, Jacinthe PA (2016) Global synthesis of drought effects on maize and wheat production. PLoS One **11**: e0156362

Dixit R, Rizzo C, Nasrallah M, Nasrallah J (2001) The *Brassica MIP-MOD* gene encodes a functional water channel that is expressed in the stigma epidermis. Plant Mol Biol **45**: 51–62

Dong J, Sun N, Yang J, Deng Z, Lan J, Qin G, He H, Deng XW, Irish VF, Chen H, et al. (2019) The transcription factors TCP4 and PIF3 antagonistically regulate organ-specific light induction of SAUR genes to modulate cotyledon opening during De-Etiolation in *Arabidopsis*. Plant Cell **31**: 1155–1170

Du Z, Zhou X, Ling Y, Zhang Z, Su Z (2010) agriGO: a GO analysis toolkit for the agricultural community. Nucleic Acids Res **38**: W64–W70

Ehlert C, Maurel C, Tardieu F, Simonneau T (2009) Aquaporin-mediated reduction in maize root hydraulic conductivity impacts cell turgor and leaf elongation even without changing transpiration. Plant Physiol 150: 1093–1104

Gupta A, Rico-Medina A, Caño-Delgado AI (2020) The physiology of plant responses to drought. Science 368: 266–269

Ishida Y, Hiei Y, Komari T (2007) Agrobacterium-mediated transformation of maize. Nat Protocol 2: 1614–1621

Jabro JD, Stevens WB, Iversen WM, Allen BL, Sainju UM (2020) Irrigation scheduling based on wireless sensors output and soil-water characteristic curve in two soils. Sensors 20: 1336

Jiao Y, Peluso P, Shi J, Liang T, Stitzer MC, Wang B, Campbell MS, Stein JC, Wei X, Chin CS, et al. (2017) Improved maize reference genome with single-molecule technologies. Nature 546: 524–527

Kakuszi A, Sarvari E, Solti A, Czegeny G, Hideg E, Hunyadi-Gulyas E, Boka K, Boddi B (2016) Light piping driven photosynthesis in the soil: low-light adapted active photosynthetic apparatus in the under-soil hypocotyl segments of bean (Phaseolus vulgaris). J Photochem Photobiol B 161: 422–429

Lee YK, Rhee JY, Lee SH, Chung GC, Park SJ, Segami S, Maeshima M, Choi G (2018) Functionally redundant LNG3 and LNG4 genes regulate turgor-driven polar cell elongation through activation of XTH17 and XTH24. Plant Mol Biol 97: 23–36

Liu H, Luo X, Niu L, Xiao Y, Chen L, Liu J, Wang X, Jin M, Li W, Zhang Q, et al. (2017) Distant eQTLs and non-coding sequences play critical roles in regulating gene expression and quantitative trait variation in maize. Mol Plant 10: 414–426

Liu S, Li C, Wang H, Wang S, Yang S, Liu X, Yan J, Li B., Beatty, M., Zastrow-Hayes, G, et al. (2020) Mapping regulatory variants controlling gene expression in drought response and tolerance in maize. Genome Biol 21: 163

Mena M, Mandel MA, Lerner DR, Yanofsky MF, Schmidt RJ (1995) A characterization of the MADS-box gene family in maize. Plant J 8: 845–854

Miao Z, Han Z, Zhang T, Chen S, Ma C (2017) A systems approach to a spatio-temporal understanding of the drought stress response in maize. Sci Rep 7: 6590

Pertea M, Kim D, Pertea GM, Leek JT, Salzberg SL (2016) Transcript-level expression analysis of RNA-seq experiments with HISAT, StringTie and Ballgown. Nat Protocol 11: 1650–1667

Ren H, Gray WM (2015) SAUR proteins as effectors of hormonal and environmental signals in plant growth. Mol Plant 8: 1153–1164

Satoh-Nagasawa N, Nagasawa N, Malcomber S, Sakai H, Jackson D (2006) A trehalose metabolic enzyme controls inflorescence architecture in maize. Nature 441: 227–230

Schmidt RJ, Veit B, Mandel MA, Mena M, Hake S, Yanofsky MF (1993) Identification and molecular characterization of ZAG1, the maize homolog of the Arabidopsis floral homeotic gene AGAMOUS. Plant Cell 5: 729–737

Schmittgen TD, Livak KJ (2008) Analyzing real-time PCR data by the comparative CT method. Nat Protocol 3: 1101

Smith AR, Zhao D (2016) Sterility caused by floral organ degeneration and abiotic stresses in Arabidopsis and cereal grains. Front Plant Sci 7: 1503

Spartz AK, Ren H, Park MY, Grandt KN, Lee SH, Murphy AS, Sussman MR, Overvoorde PJ, Gray WM (2014) SAUR inhibition of PP2C-D phosphatases activates plasma membrane H+-ATPases to promote cell expansion in Arabidopsis. Plant Cell 26: 2129–2142

Sun H, Wang C, Chen X, Liu H, Huang Y, Li S, Dong Z, Zhao X, Tian F, Jin W (2020) dlf1 promotes floral transition by directly activating ZmMADS4 and ZmMADS67 in the maize shoot apex. New Phytol 228: 1386–1400

Sun N, Wang J, Gao Z, Dong J, He H, Terzaghi W, Wei N, Deng XW, Chen H (2016) Arabidopsis SAURs are critical for differential light regulation of the development of various organs. Proc Natl Acad Sci USA 113: 6071–6076

Tanaka W, Pautler M, Jackson D, Hirano HY (2013) Grass meristems II: inflorescence architecture, flower development and meristem fate. Plant Cell Physiol 54: 313–324

Theißen G, Strater T, Fischer A, Saedler H (1995) Structural characterization, chromosomal localization and phylogenetic evaluation of two pairs of AGAMOUS-like MADS-box genes from maize. Gene 156: 155–166

Thimm O, Bläsing O, Gibon Y, Nagel A, Meyer S, Krüger P, Selbig J, Müller LA, Rhee SY, Stitt M (2004) MAPMAN: a user-driven tool to display genomics data sets onto diagrams of metabolic pathways and other biological processes. Plant J. 37: 914–939

Thompson BE, Hake S (2009) Translational biology: from Arabidopsis flowers to grass inflorescence architecture. Plant Physiol 149: 38–45

Thompson BE, Bartling L, Whipple C, Hall DH, Sakai H, Schmidt R, Hake S (2009) bearded-ear encodes a MADS box transcription factor critical for maize floral development. Plant Cell 21: 2578–2590

Tian T, Liu Y, Yan H, You Q, Yi X, Du Z, Xu W, Su Z (2017) agriGO v2.0: a GO analysis toolkit for the agricultural community, 2017 update. Nucleic Acids Res 45: W122–W129

Usadel B, Poree F, Nagel A, Lohse M, Czedik-Eysenberg A, Stitt M (2009) A guide to using MapMan to visualize and compare Omics data in plants: a case study in the crop species, Maize. Plant Cell Environ 32: 1211–1229

Verbancic J, Lunn JE, Stitt M, Persson S (2018) Carbon supply and the regulation of cell wall synthesis. Mol Plant 11: 75–94

Vollbrecht E, Springer PS, Goh L, Buckler EST, Martienssen R (2005) Architecture of floral branch systems in maize and related grasses. Nature 436: 1119–1126

Wang X, Wang H, Liu S, Ferjani A, Li J, Yan J, Yang X, Qin F (2016) Genetic variation in ZmVPP1 contributes to drought tolerance in maize seedlings. Nat Genet 48: 1233–1241

Wu Y, Jeong BR, Fry SC, Boyer JS (2005) Change in XET activities, cell wall extensibility and hypocotyl elongation of soybean seedlings at low water potential. Planta 220: 593–601

Yang N, Liu J, Gao Q, Gui S, Chen L, Yang L, Huang J, Deng T, Luo J, He L, et al. (2019) Genome assembly of a tropical maize inbred line provides insights into structural variation and crop improvement. Nat Genet 51: 1052–1059

Yeung KY, Haynor DR, Ruzzo WL (2001) Validating clustering for gene expression data. Bioinformatics 17: 309–318

Zhou LZ, Juranic M, Dresselhaus T (2017) Germline development and fertilization mechanisms in maize. Mol Plant 10: 389–401

Zhu JK (2016) Abiotic stress signaling and responses in plants. Cell 167: 313–324